Selective Recognition and Cleavage of RNA Loop Structures by Ni(II)·Xaa-Gly-His Metallopeptides†

Isabelle J. Brittain, Xiaofen Huang, and Eric C. Long*

Department of Chemistry, Indiana University Purdue University−Indianapolis, Indianapolis, Indiana 46202-3274

Received March 23, 1998; Revised Manuscript Received July 8, 1998

ABSTRACT: The recognition and cleavage of $tRNA^{Phe}$ and the TAR RNA of HIV-1 by metallopeptides of the general form Ni(II)·Xaa-Gly-His (where Xaa is Gly, Lys, or Arg) were investigated. The results of RNA cleavage analyses suggest that $KHSO_5$- or magnesium monoperoxyphthalate-activated metallopeptides (1) induce nucleobase damage which requires aniline acetate for complete RNA strand scission and (2) selectively target the loops of stem−loop structures of the above-named substrates. In targeting RNA loop regions, the metallopeptides may be sensitive to intraloop structural features, including the overall structural environment of the loop itself and possibly the presence of intraloop hydrogen bonding. Overall, these results suggest that the metallopeptides interact selectively within a loop, in a fashion reminiscent of many RNA binding proteins, instead of targeting RNA single-stranded character alone. These observations further suggest a possible metallopeptide-based strategy for the molecular recognition of native RNA structures and insight with regard to the general features available for ligand binding site discrimination.

Understanding the molecular recognition and chemical modification of RNA by low-molecular weight molecules has become a topic of significant current interest (*1*). While our present level of knowledge concerning RNA−small molecule interactions does not yet parallel our same understanding of DNA, a drive to develop and study these interactions is spurred by the use of low-molecular weight molecules as probes of RNA structure and function (*1*−*3*). In addition, an increased understanding of RNA−small molecule interactions may lead to the development of novel chemotherapeutic agents for blocking the natural function(s) of an RNA, especially in organisms that rely upon unique RNA−macromolecule interactions or upon RNA as a genetic material (e.g., HIV-1[1]).

As is also the case with DNA (*2*, *3*), low-molecular weight metal complexes have the potential to assist in our understanding of RNA molecular recognition events; such agents can provide unique, geometrically defined structures to complement the rich diversity of three-dimensional shapes provided by a structured RNA. Indeed, it is more likely that the selective targeting of an RNA will be based on its overall structure rather than its sequence of nucleotides (*1*). In addition, a metal center can also impart redox properties to an otherwise unreactive ligand, resulting in an agent with the ability to bind and modify a target nucleic acid. Currently, there are several metal complexes (*1*), both naturally occurring and wholly synthetic, that have increased our knowledge of the molecular recognition of RNA, its solution structure(s), and chemical reactivity. Examples include Fe(II)·bleomycin (*4*−*6*), octahedral complexes of Rh(III) (*7*, *8*), square-planar Ni(II) complexes (*9*, *10*), and bis(1,10-phenanthroline)copper(I) (*3*, *11*).

Recently, our laboratories have exploited the use of metallopeptides to further the understanding of small molecule−DNA interactions (*12*−*14*). We have demonstrated that metallopeptides of the general form Ni(II)·Xaa-Xaa-His (where Xaa-Xaa-His is NH_2-Xaa-Xaa-His-$CONH_2$ and Xaa is an α amino acid) have the ability to bind and, when appropriately activated (*14*), mediate the selective strand scission of DNA (Figure 1) (*12*); selective DNA cleavage occurs through a judicious choice of the composition and chirality of the amino acids included in the tripeptide ligand. Given their use of amino acids, Ni(II)·Xaa-Xaa-His metallopeptides are unique in their ability to incorporate and position within a metal complex framework the same chemical functionalities (e.g., guanidinium, amide, or amine moieties) used by proteins and natural products for the molecular recognition of DNA and RNA (*15*, *16*). These features, therefore, make Ni(II)·Xaa-Xaa-His metallopeptides attractive models for furthering our understanding of small molecule−RNA recognition principles.

Described herein is an examination of Ni(II)·Xaa-Gly-His metallopeptide interactions (where Xaa is Gly, Lys, or Arg) with $tRNA^{Phe}$ and the TAR RNA of HIV-1. The findings indicate that Ni(II)·Xaa-Gly-His metallopeptides selectively

† This research was supported by a grant from the National Institutes of Health (GM50557).

* To whom correspondence should be addressed at the Department of Chemistry, Indiana University Purdue University−Indianapolis, 402 N. Blackford St., Indianapolis, IN 46202-3274. E-mail: long@chem.iupui.edu. Telephone: (317) 274-6888. Fax: (317) 274-4701.

[1] Abbreviations: FAB-MS, fast atom bombardment mass spectrometry; HIV-1, human immunodeficiency virus type 1; MMPP, magnesium monoperoxyphthalate; mRNA, messenger RNA; NiCR, (2,12-dimethyl-3,7,11,17-tetraazabicyclo[11.3.1]heptadeca-1(17),2,11,13,15-pentaenato)nickel(II) perchlorate; TAR, trans-activating response element; TAT, transcription antitermination; tRNA, transfer RNA; Xaa, α-amino acid.

S0006-2960(98)00660-6 CCC: $15.00
Published on Web 08/12/1998

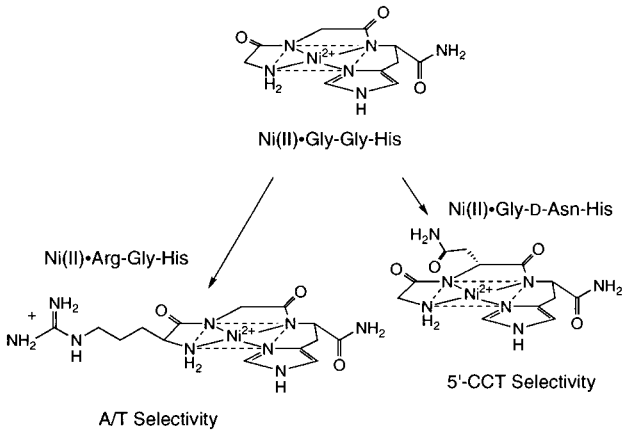

FIGURE 1: Representative Ni(II)•Xaa-Xaa-His metallopeptides active in nucleic acid strand scission.

cleave within the single-stranded hairpin loops of these RNAs. These data suggest that the metallopeptide framework may partially insert into an RNA loop, resulting in damage to the nucleobases (*17*) located in the proximity of the metal center of the bound complex. Given their selectivity for loop structures, the metallopeptides appear to mimic the behavior of many sequence-selective RNA binding proteins (*15*, *16*). Importantly, these findings indicate that metallopeptides may provide a unique means of selectively recognizing and/or probing the structures of native RNA hairpin loops which could complement strategies currently available (*1*).

EXPERIMENTAL PROCEDURES

Materials. Native yeast $tRNA^{Phe}$ was purchased from Sigma. TAR RNA was provided by D. Mack of Parke-Davis Pharmaceuticals. TAR DNA was purchased from Genemed Synthesis (San Fransisco, CA). All buffer solutions were made with Milli-Q purified water, treated with diethyl pyrocarbonate, and autoclaved. All other reagents and enzymes were obtained RNase-free and in the highest grades commercially available. [5′-^{32}P]Cytidine 3′,5′-bisphosphate (pCp) was purchased from ICN Biomedicals, Inc. All protected amino acids for peptide syntheses were purchased from Bachem California. Peptide syntheses were carried out by conventional solid-phase methodologies (*18*) followed by reverse-phase HPLC purification and verification by FAB-MS.

Preparation of ^{32}P End-Labeled RNAs. Yeast $tRNA^{Phe}$ and TAR RNA were 3′-^{32}P end-labeled in 20 μL total volumes containing 15 pmol of RNA, 2 μL of neat DMSO, and 5 μL of [5′-^{32}P]pCp. Added to these mixtures was 5 μL of a dilute enzyme solution containing 2 μL of T4 RNA ligase (47.6 units) and 20 μL of a ligase buffer [consisting of 200 μL of Tris•HCl (pH 7.5), 40 μL of $MgCl_2$, 80 μL of 1 M DTT, 40 μL of 100 mM ATP, 20 μL of BSA (20 mg/mL), and 620 μL of H_2O]. Reaction mixtures were incubated for 2 h at 4 °C. The resulting RNAs were purified on 15% denaturing polyacrylamide gels, located by autoradiography, excised, and eluted from the gel material in TE buffer (pH 7.4). The eluted RNAs were desalted using a Nensorb column and renatured by slow cooling overnight to 25 °C from an initial temperature of 65 °C in 10 mM sodium cacodylate/10 mM $MgCl_2$ buffer (pH 7.0) ($tRNA^{Phe}$) or 10 mM sodium cacodylate buffer (pH 7.0) (TAR RNA).

RNA Cleavage Reactions. Metallopeptide-induced cleavage reactions were carried out in 20 μL total volumes containing carrier yeast tRNA (100 μM nucleotide concentration) and 4×10^4 cpm of 3′-^{32}P end-labeled RNA in 10 mM sodium cacodylate/10 mM $MgCl_2$ buffer (pH 7.0) ($tRNA^{Phe}$) or 10 mM sodium cacodylate buffer (pH 7.0) (TAR RNA). Reactions were initiated through the admixture of RNA and equimolar amounts of preformed Ni(II)•peptide and $KHSO_5$ (oxone) and quenched after 1 min with the addition of 3 μL of a 0.2 M EDTA solution. All reaction mixtures were ethanol precipitated with the addition of 10 μL of 3 M sodium acetate and 130 μL of cold EtOH overnight. The precipitated RNA was washed with 100 μL of 80% EtOH, dried, and treated with aniline acetate (*19*). All reaction mixtures, along with RNA sequencing reaction mixtures (*19*), were heat-denatured at 90 °C for 5 min and quick-chilled on ice. The samples were loaded onto 20% (19:1) polyacrylamide/7.5 M urea sequencing gels and electrophoresed at 600 V overnight. Gels were transferred to an autoradiography cassette and exposed to Kodak X-omat film at −70 °C.

TAR DNA Cleavage Reactions. Metallopeptide-induced cleavage reactions were carried out in a 20 μL total volume containing 50 μM (nucleotide concentration) calf thymus DNA and 3×10^4 cpm of 3′-^{32}P end-labeled TAR DNA in 10 mM sodium cacodylate buffer (pH 7.0) at 4 °C. Reactions were initiated through the admixture of DNA and equimolar amounts of Ni(II)•peptide and $KHSO_5$ (oxone) and quenched after 1 min with 4 μL of a 0.2 M EDTA solution. Following EtOH precipitation, the DNA pellets were treated with 0.1 M *n*-butylamine at 90 °C for 15 min and dried. All reaction mixtures, along with DNA sequencing reaction mixtures, were heat-denatured at 90 °C for 5 min and quick-chilled on ice. The samples were loaded onto 20% polyacrylamide/7.5 M urea denaturing gels and electrophoresed at 600 V overnight. Autoradiography of the gel was conducted at −70 °C using Kodak X-omat film.

RESULTS

Metallopeptide Cleavage of $tRNA^{Phe}$. The result of a high-resolution polyacrylamide gel analysis of the cleavage of native $tRNA^{Phe}$ by Ni(II)•Xaa-Gly-His metallopeptides is shown in Figure 2. While the immediate reaction between $KHSO_5$-activated metallopeptides (*14*) and 3′-^{32}P end-labeled $tRNA^{Phe}$ did not result in RNA cleavage, strand scission was observed after treatment of each reaction with aniline acetate; this treatment appears, although this is not definitive at present, to produce fragmented RNA bearing 5′-phosphorylated termini as evidenced by their comigration with the products of nucleobase-modifying sequencing reactions (*20*).

Upon aniline acetate treatment, the gel analysis in Figure 2 revealed the selective cleavage of 3′-^{32}P end-labeled $tRNA^{Phe}$ by Ni(II)•Gly-Gly-His (lanes 2−4), Ni(II)•Lys-Gly-His (lanes 5−7), and Ni(II)•Arg-Gly-His (lanes 8−10). The cleavage induced by the metallopeptides, in comparison to RNA sequencing lanes, occurred at a variety of nucleobases, including A, G, C, U, and the modified Y and Ψ nucleobases. This observation demonstrated that the cleavage selectivity of the metallopeptides was not nucleobase-specific. In addition, it was also observed that all of the metallopeptides induced similar (1) amounts of total RNA degradation and

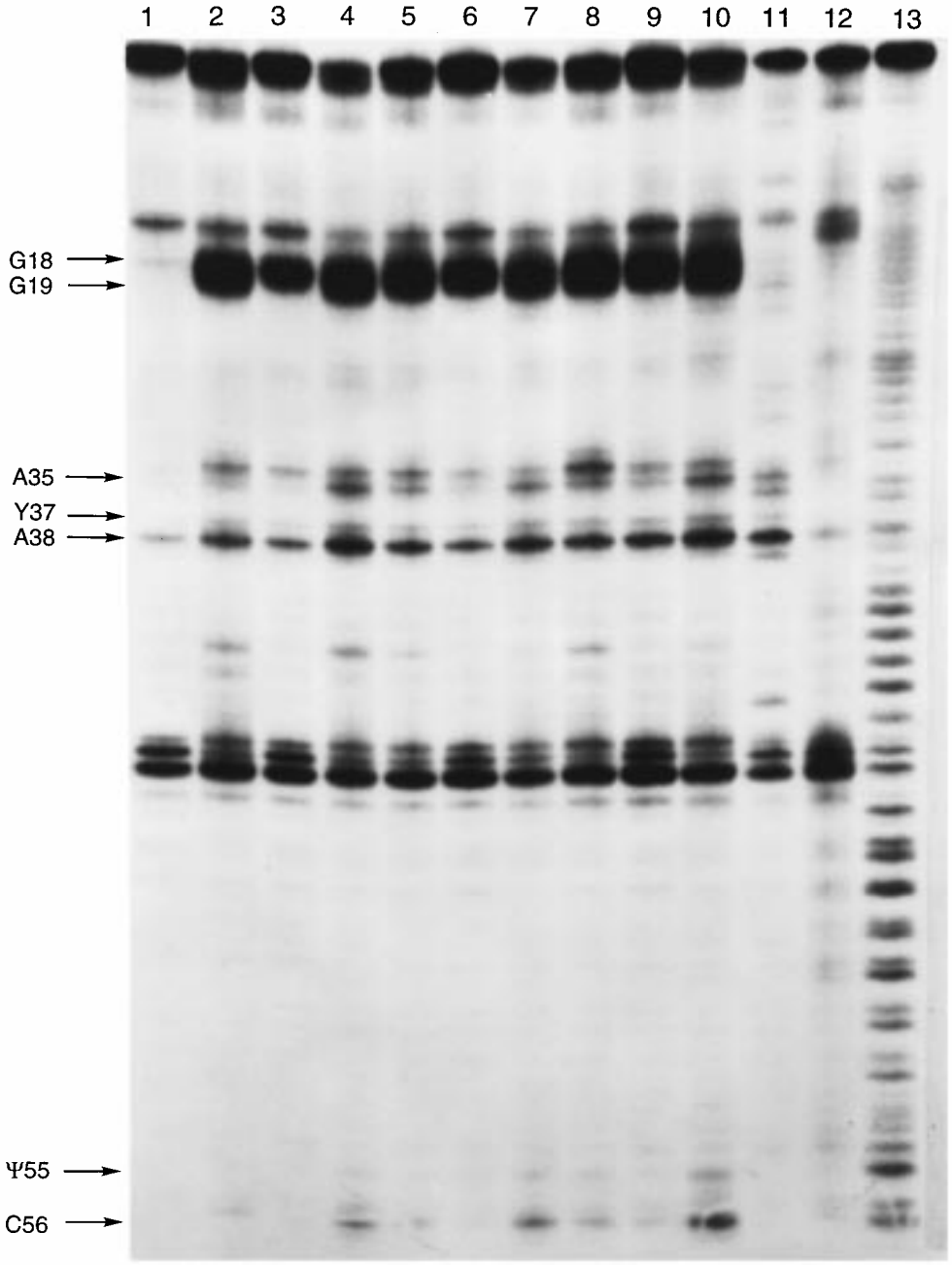

FIGURE 2: Cleavage of native tRNA^{Phe} by Ni(II)·Xaa-Gly-His metallopeptides. End-labeled tRNA^{Phe} was treated with one of the Ni(II)·Xaa-Gly-His metallopeptides followed by aniline acetate treatment as described in Experimental Procedures. All lanes contained 100 μM (nucleotide concentration) yeast tRNA: lane 1, control reaction, 500 μM Ni(II)·acetate and 500 μM $KHSO_5$; lanes 2−4, 100, 250, and 500 μM Ni(II)·Gly-Gly-His/$KHSO_5$, respectively; lanes 5−7, 100, 250, and 500 μM Ni(II)·Lys-Gly-His/$KHSO_5$, respectively; lanes 8−10, 100, 250, and 500 μM Ni(II)·Arg-Gly-His/$KHSO_5$, respectively; lane 11, A>G sequencing reaction; lane 12, U-specific sequencing reaction; and lane 13, alkaline hydrolysis reaction.

(2) cleavage selectivities despite differences in their charges and amino-terminal Xaa composition under the conditions employed.

The sites of tRNA^{Phe} cleavage produced by the metallopeptides are summarized using the cloverleaf depiction shown in Figure 3. Each metallopeptide induced the selective scission of the loop regions of tRNA^{Phe} at micromolar concentrations, within (1) the D loop (G18 and G19), (2) the anticodon loop (A35, Y37, and A38), and (3) the TΨC loop (Ψ55, C56, U59, and C61) (cleavage at U59 and C61 is not visible in Figure 2). Overall, the metallopeptides exhibited a strong preference for loops and were not observed to cleave the double-stranded regions of tRNA^{Phe} or any single-stranded regions not involved in stem−loop structures (i.e., the acceptor stem).

Along with the sites of cleavage mentioned above, low levels of tRNA^{Phe} cleavage were also observed at Gm34, G43, and A44; these acts of cleavage were not, however, observed to occur consistently as a function of metallopeptide concentration. In addition to the metallopeptide-dependent cleavage described in the previous paragraph, tRNA^{Phe} hydrolysis was also observed at A14, U47, and C48 solely as a function of aniline acetate treatment.

Metallopeptide Cleavage of TAR RNA. The result of a high-resolution polyacrylamide gel analysis of the cleavage of HIV-1 TAR RNA by Ni(II)·Xaa-Gly-His metallopeptides

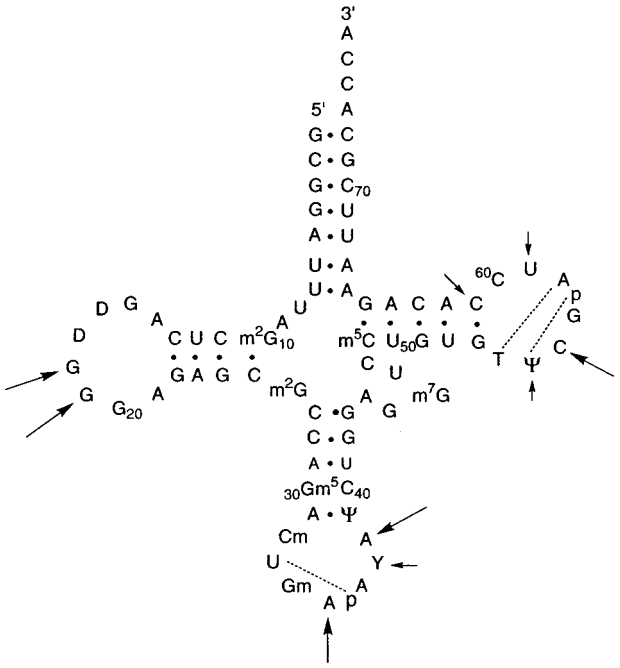

FIGURE 3: Secondary structure of tRNA^{Phe}. The arrows denote the sites of cleavage induced by Ni(II)·Xaa-Gly-His metallopeptides; arrow length is directly proportional to the cleavage intensity observed at a given site. Dashed lines indicate the locations of documented intraloop hydrogen bonding.

is shown in Figure 4. TAR RNA was cleaved by Ni(II)·Gly-Gly-His (lanes 4−6), Ni(II)·Lys-Gly-His (lanes 7−9), and Ni(II)·Arg-Gly-His (lanes 10−12) at micromolar concentrations upon aniline acetate treatment; as with tRNA^{Phe}, cleavage was not observed in the absence of aniline acetate. As summarized in Figure 5, the cleavage of TAR RNA occurred in the apical loop region at residues G32, G33, G34, A35, and G36. Given the cleavage at both A and G residues, the metallopeptides, as with tRNA^{Phe}, were not found to be nucleobase-specific and to exhibit identical cleavage selectivities, despite their structural differences. In addition to cleavage of the apical loop, very low, yet detectable levels of cleavage were also noted within the A-form stem of TAR RNA; as illustrated in Figures 4 and 5, residues C41, G43, and G44 were recognized and cleaved by the metallopeptides. In addition to $KHSO_5$ activation, metallopeptide activation with MMPP (*14*) resulted in identical site-selective cleavage of TAR RNA upon aniline acetate treatment (data not shown).

In contrast, however, to several agents which have been examined with TAR RNA (*21*−*24*), the Ni(II)·Xaa-Gly-His metallopeptides were not found to interact with or cleave the bulge region. This was further probed by competition studies with argininamide (data not shown); Ni(II)·metallopeptide-induced cleavage of the apical loop of TAR was not inhibited by the presence of argininamide (100 μM to 2 mM) which binds to the bulge region within this concentration range (*25*, *26*).

Metallopeptide Cleavage of TAR DNA. A summary of the results of high-resolution polyacrylamide gel analyses of the cleavage of TAR DNA by Ni(II)·Gly-Gly-His, Ni(II)·Lys-Gly-His, and Ni(II)·Arg-Gly-His is shown in Figure 6. TAR DNA was cleaved to a similar extent and with similar selectivities by all three metallopeptides within the concentration range that was employed. Direct DNA strand scission was observed; however, this cleavage was enhanced upon treatment of reaction mixtures with *n*-butylamine (*14*) which is known to assist in the breakdown of abasic lesions produced upon C4′-hydroxylation of a targeted nucleotide. As shown in Figure 6, the cleavage of TAR DNA occurred (using the same nucleotide numbering scheme as employed with TAR RNA) at (1) the three-nucleobase bulge (T25), (2) the stem connecting the bulge and apical loop (G26, A27, G28, and C39), and (3) the apical loop (T31, G32, G33, and G34). In addition, a moderately strong cleavage site was also observed at G43.

DISCUSSION

We employed Ni(II)·Gly-Gly-His, Ni(II)·Lys-Gly-His, and Ni(II)·Arg-Gly-His as cleavage reagents in our initial studies of RNA−metallopeptide interactions. These metallotripeptides were chosen due to their amino acid composition; Ni(II)·Gly-Gly-His represents the simplest, unsubstituted complex, while Ni(II)·Lys-Gly-His and Ni(II)·Arg-Gly-His were chosen for their positively charged Lys and Arg side chains. By analogy to their interactions with DNA, the positive charge on the side chains of Lys and Arg should increase the affinity of their respective metallopeptides for the polyanionic RNA backbone (*12*). In addition, Arg- and Lys-containing peptides were chosen to permit the inclusion of amino acids known to mediate protein interactions with RNA (*15*, *16*).

Initially, the well-characterized RNA tRNA^{Phe} was employed as a substrate in its native conformation. This transfer RNA is frequently chosen as a substrate because the availability of its crystal structure (*27*, *28*) makes it possible to correlate sites of small molecule interaction and/or cleavage with details of RNA structure. The second substrate employed in this investigation was the TAR RNA of HIV-1, a hairpin structure found at the 5′-termini of all HIV-1 viral mRNAs (*29*, *30*). This unique RNA structure, with its bulge, apical loop, and A-form stem, offers another target for testing the RNA recognition exhibited by the metallopeptides. In addition, the bulge of TAR RNA is known to furnish a binding site for the interaction of many low-molecular weight molecules (*21*−*24*), including Arg and Arg analogues, via their guanidinium groups (*31*, *32*); the Arg-containing metallopeptides could therefore have facilitated a selective targeting of the bulge region.

Chemistry of Metallopeptide-Induced RNA Cleavage. The metallopeptide-induced cleavage of tRNA^{Phe} and TAR RNA required a postreaction aniline acetate treatment to induce strand scission of the biopolymer backbone. No biopolymer cleavage occurred without this base treatment, as is also observed with the nucleobase-specific sequencing reactions employed in this study (*19*, *20*). These observations suggest that the predominant means of metallopeptide-induced RNA damage occurs through initial nucleobase modification followed by complete strand scission only upon aniline acetate treatment.

An examination of the sites of cleavage of tRNA^{Phe} and TAR RNA also demonstrated that the cleavage induced by the metallopeptides was not nucleobase-selective, since cleavage occurred at a variety of sites, including A, G, C, Ψ, and the modified Y nucleobases. In contrast to other Ni complexes, e.g., NiCR (*9*), a specificity for G residues alone

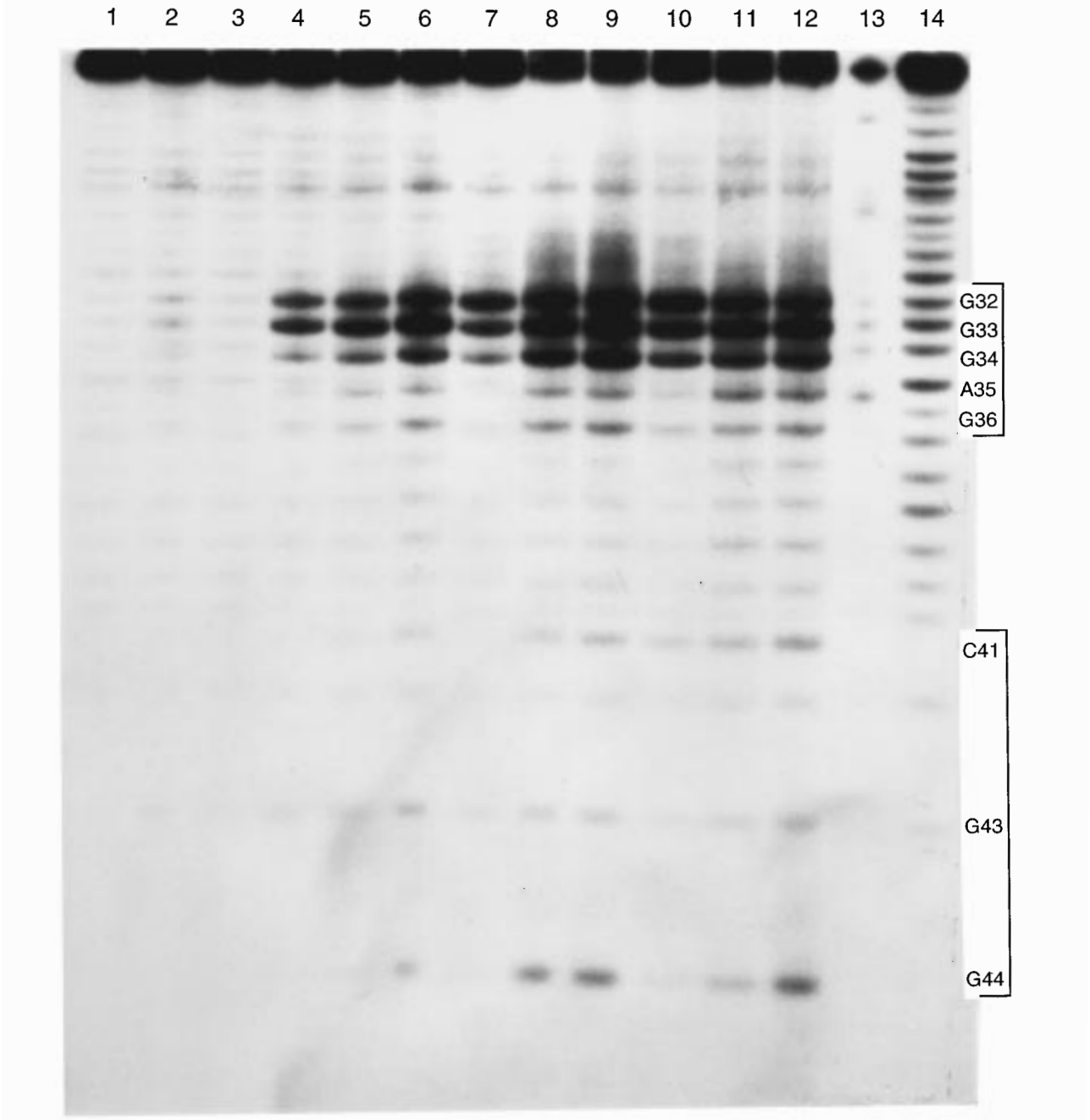

FIGURE 4: Cleavage of the TAR RNA of HIV-1 by Ni(II)·Xaa-Gly-His metallopeptides. End-labeled $tRNA^{Phe}$ was treated with one of the Ni(II)·Xaa-Gly-His metallopeptides followed by aniline acetate treatment as described in Experimental Procedures. All lanes contained 100 μM (nucleotide concentration) yeast tRNA: lane 1, TAR RNA alone; lane 2, control reaction, 500 μM Ni(II)·Gly-Gly-His; lane 3, control reaction, 500 μM Ni(II)·acetate and 500 μM $KHSO_5$; lanes 4−6, 250 μM, 500 μM, and 1 mM Ni(II)·Gly-Gly-His/$KHSO_5$, respectively; lanes 7−9, 250 μM, 500 μM, and 1 mM Ni(II)·Lys-Gly-His/$KHSO_5$, respectively; lanes 10−12, 250 μM, 500 μM, and 1 mM Ni(II)·Arg-Gly-His/$KHSO_5$, respectively; lane 13, A>G sequencing reaction; and lane 14, alkaline hydrolysis reaction.

was not observed with the conditions and concentrations employed, suggesting differences in (1) the chemistry of the "activated" complexes formed or (2) the extent of their noncovalent interaction with a target RNA. It appears likely that NiCR directly metalates surface-accessible guanine residues (via N7) leading to their preferential oxidation (*9*, *10*), while the noncovalent preassociation of the Ni(II)·metallopeptides with an RNA loop may result in the oxidation of nucleobases which are positioned in close proximity to the metal center of an "activated metallopeptide" (*14*). In addition, it is also quite likely that the metallopeptides induce some nucleobase damage (*14*) in a fashion similar to that of NiCR (*9*) at highly exposed guanine residues within $tRNA^{Phe}$ (e.g., G18 and G19 of the D-loop).

For comparison to the above, with B-form DNA, noncovalent preassociation of an activated Ni(II)·metallopeptide in the minor groove leads to C4′−H abstraction of a target deoxyribose. This initial C−H bond abstraction results in direct DNA strand scission via a C4′-hydroperoxide intermediate or alkaline-labile site formation via a C4′-hydroxylated nucleotide (*14*). In addition to deoxyribose modification, under conditions of increased ionic strength or excess activating agent ($KHSO_5$), the metallopeptides can also mediate guanine nucleobase oxidation (*14*). Overall, the somewhat more stringent reaction conditions required for RNA cleavage (i.e., aniline acetate treatment and elevated

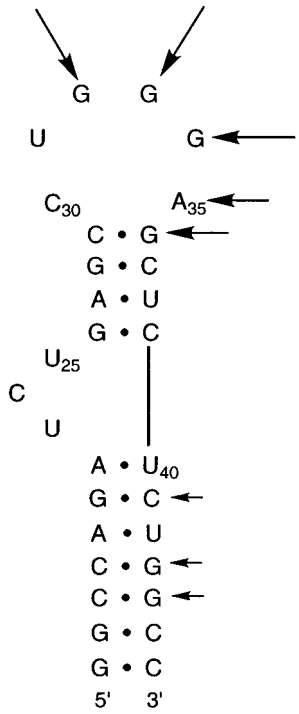

FIGURE 5: Secondary structure of the TAR RNA of HIV-1. The arrows denote the sites of cleavage by Ni(II)·Xaa-Gly-His metallopeptides; arrow length is directly proportional to the cleavage intensity observed at a given site.

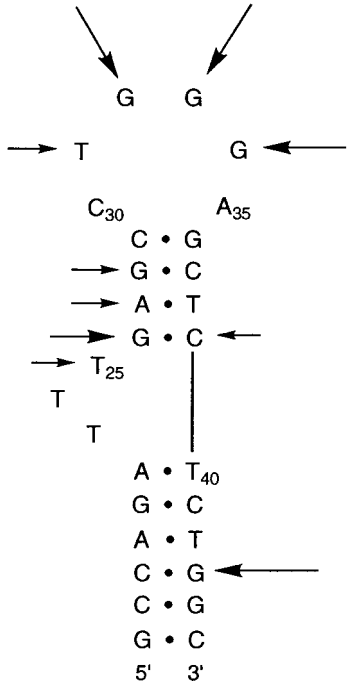

FIGURE 6: Secondary structure of TAR DNA. The arrows denote the sites of cleavage by Ni(II)·Xaa-Gly-His metallopeptides; arrow length is directly proportional to the cleavage intensity observed at a given site.

metallopeptide concentrations) versus DNA cleavage by the metallopeptides likely reflect the predominance of nucleobase-centered chemistry as opposed to sugar-based chemistry.

Site-Selective Cleavage of Native tRNA^{Phe}. Each metallopeptide employed in this study was capable of cleaving the single-stranded hairpin loop structures of native tRNA^{Phe} (Figure 7). Surprisingly, despite the conditions necessary to maintain the native structure of this substrate (10 mM $MgCl_2$), the metallopeptides still produced selective RNA modification at concentrations similar to those employed with Fe(II)·bleomycin (*5*). Apparently, the charge differences between the metallopeptides did not significantly influence their ability to cleave native tRNA^{Phe}. By analogy to DNA (*12*), the neutral complex Ni(II)·Gly-Gly-His was expected to show less affinity for the polyanionic tRNA^{Phe} compared to the positively charged complexes Ni(II)·Lys-Gly-His and Ni(II)·Arg-Gly-His; the conditions necessary to maintain the native tRNA structure may have effectively screened any electrostatic contribution to metallopeptide−RNA binding. However, this observation also suggests that common elements of the basic metallopeptide framework may recognize and bind to the loop structures of tRNA^{Phe} regardless of the moiety appended to the α-carbon of the N-terminal amino acid residue. In addition, the above results also indicate that the metallopeptides were unable to cleave duplex regions of tRNA^{Phe} as they do via the minor groove of duplex DNA; this is as expected given the inaccessible structure of these corresponding grooves in duplex RNA (*15*, *16*, *33*, *34*).

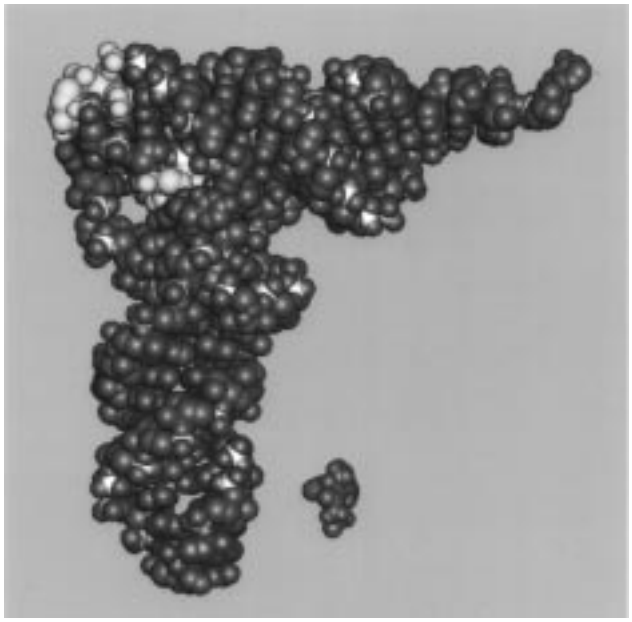

FIGURE 7: Structure of tRNA^{Phe} highlighting the locations of Ni(II)·Xaa-Gly-His metallopeptide-induced cleavage. Cleavage sites (nucleotides) in the anticodon, TΨC, and D-loops are green, yellow, and red, respectively. For comparison, the structure of a Ni(II)·Xaa-Gly-His metallopeptide is located adjacent to the anticodon loop to emphasize their structural complementarity and a possible location of metallopeptide binding.

A close examination of the metallopeptide-induced cleavage pattern of tRNA^{Phe} indicates that the majority of the cleavage sites induced by all three complexes occurred consistently within the 3′-half of the TΨC and anticodon loops, suggesting a distinct orientation of the metallopeptide upon loop binding. Differing from several reagents known to interact with single-stranded RNA structures (*11*, *35*), the metallopeptides appear to interact selectively within an individual loop instead of reacting with its single-stranded character alone. This metallopeptide selectivity could possibly be enhanced by the presence of a defined structure within the targeted hairpin loops.

Previously, structural investigations have revealed a unique feature within the anticodon and TΨC loops of tRNA^{Phe} (*27*, *28*); these loops are involved in the formation of "uridine

turns" (U-turns), where the U residues in these loops are hydrogen-bonded to a phosphate on the opposite side of the loop in the consensus sequence UNR (where N is any nucleotide and R is a purine residue) (*36*). In the anticodon loop, this consensus sequence contains U33-Gm34-A35, with U33 hydrogen-bonded to P36, while in the TΨC loop, the consensus sequence includes residues Ψ55-C56-G57 with Ψ55 interacting with P58. Curiously, the nucleotides immediately adjacent to the phosphates involved in U-turn formation in the anticodon and TΨC loops (i.e., P36 and P58, respectively) are not cleaved by the metallopeptides (Figure 3). While only a working hypothesis at this point, this observation suggests that the metallopeptides might be capable of sensing subtle, intraloop structural features such as the hydrogen bonding pattern required for U-turn formation.

Interestingly, close examination of molecular models of the anticodon and TΨC loops of $tRNA^{Phe}$ reveals a possible metallopeptide binding site. This binding "pocket" can be envisioned in the center of these loops where the square-planar metallopeptide can be inserted with the side chain of the terminal residue pointed outward to facilitate interactions with the phosphate backbone (Figure 7); this model of loop recognition (1) is compatible with data which indicate that substitution at the terminal α-carbon of the metallopeptide does not affect loop cleavage and (2) parallels the model of metallopeptide−DNA minor groove association (*12*). The selective metallopeptide-induced cleavage of the anticodon and TΨC loops in $tRNA^{Phe}$ suggests that a structured loop region might facilitate the recognition and binding of a metallopeptide or allow discrimination among ligands, in general.

Increased knowledge of the diversity of selective $tRNA^{Phe}$ binding and cleaving reagents has assisted in our understanding of RNA recognition principles. In comparison to other reagents, the metallopeptides are unique in the fact that they appear to recognize and cleave hairpin loop structures selectively and to perhaps sense their local environment and conformation. For comparison, several members of the family of enediyne antibiotics are also known to cleave $tRNA^{Phe}$ within single-stranded loop regions (*35*). However, in contrast to Ni(II)·Xaa-Gly-His metallopeptides, the presence of a native $tRNA^{Phe}$ structure, or the conditions necessary to achieve a native structure, dramatically diminish the cleavage exhibited by these reagents. In addition, $Cu(phen)_2^+$ recognizes single-stranded regions and the double-stranded acceptor stem of $tRNA^{Phe}$, quite possibly through interactions between the phenanthroline ligands of this complex and unstacked nucleobases (*11*).

Along with the complexes discussed above, other transition metal complexes also recognize $tRNA^{Phe}$ and additional RNAs on the basis of structure rather than sequence: (1) $Rh(phen)_2phi^{3+}$ induces cleavage at residues in opened major grooves, as occurs at triply bonded bases within $tRNA^{Phe}$ (*7*, *8*), (2) the antitumor antibiotic Fe(II)·bleomycin exhibits a preference for junctions between single- and double-stranded regions in $tRNA^{Phe}$ (*4*−*6*), and (3) oxoruthenium intercalators (*37*, *38*) can target unique sites within $tRNA^{Phe}$ and ferritin mRNA. Overall, the activities of the above complexes highlight the unique nature of the cleavage of $tRNA^{Phe}$ by Ni(II)·Xaa-Gly-His metallopeptides.

Site-Selective Cleavage of TAR RNA. The site-selective cleavage of TAR RNA indicates, as is also the case with $tRNA^{Phe}$, that the metallopeptides recognize and cleave predominantly within the 3′-half of the single-stranded apical loop of this substrate. While the apical loop of TAR RNA does not contain a documented U-turn (*25*, *26*, *30*), structural investigations (*39*, *40*) and the use of molecular probes (*23*, *38*) have indicated that the apical loop of TAR presents a partially ordered RNA region capable of binding intercalators. Accordingly, this investigation suggests that the metallopeptides may be specifically recognizing an open, accessible structure in the loop region of TAR RNA that is also capable of binding intercalators (*38*). Again, a pattern of metallopeptide-induced loop cleavage that occurs toward the 3′-side of TAR RNA is observed in this and all stem−loop substrates that were examined and may reflect the common property of their attachment to a chiral A-form helical stem; i.e., the "chiral" curvature of the loop directs the insertion and orientation of a noncovalently bound metallopeptide.

Surprisingly, in comparison to other TAR RNA binding and cleaving agents examined to date, the metallopeptides are unique in that they do not cleave the bulge region. It was originally thought that, due to its guanidinium group, Ni(II)·Arg-Gly-His would perhaps interact with the bulge region of TAR as found for free Arg or Arg analogues. These results, however, indicate that this was not the case. All three metallopeptides exhibited the same site selectivity for TAR RNA. This finding was further substantiated by the fact that metallopeptide cleavage of the loop region of TAR RNA was not inhibited in the presence of argininamide over a wide concentration range (100 μM to 2 mM). Argininamide, as well as free arginine, is known to bind within the bulge region with a K_d of 2−3 mM (*25*, *26*). Therefore, metallopeptide binding does not appear to (1) involve the major groove of the bulge or (2) be affected by the conformational changes that occur upon Arg·TAR complexation (*30*). However, a slight amount of cleavage was observed within the A-form stem (C41, G43, and G44) at the higher concentrations of metallopeptide that were employed, suggesting that the altered groove width of this region of TAR RNA (*41*) may provide a low-affinity site for metallopeptide binding.

For comparison to the results obtained with TAR RNA, the DNA analogue of this substrate (TAR DNA) was also employed in metallopeptide cleavage reactions. The results obtained with this substrate indicate that Ni(II)·Xaa-Gly-His metallopeptides, in a fashion similar to those of other reagents that have cleaved TAR DNA (*24*, *38*), are now capable of targeting the bulge, apical loop, and B-form stem connecting these two regions. While cleavage of the apical loops of both the RNA and DNA substrates is observed, fundamental differences between their patterns of modification result; with TAR RNA, loop cleavage occurs toward the 3′-side as with other RNA loops, while with TAR DNA, cleavage occurs predominantly at the apex of the DNA loop. These cleavage patterns, while obviously reflecting conformational differences between a DNA and RNA substrate, suggest that the cleavage of the 3′-side of RNA loops may be an inherent outcome of their interaction with Ni(II)·Xaa-Gly-His metallopeptides.

To date, several classes of TAR RNA bulge-selective agents have been discovered; these agents include the tetrahydropyrimidines (*21*), arginine analogues (*32*), aminoglycoside antibiotics (*22*), the enediyne antitumor antibiotics (*24*), and $Rh(phen)_2phi^{3+}$ (*23*). Each of these agents has shown the ability to bind to TAR RNA via the opened major groove in the bulged region. Curiously, the metallopeptides do not recognize this feature of TAR RNA. Perhaps this structure cannot sterically complement Ni(II)·Xaa-Gly-His binding, whereas loops of larger size, or containing some level of a defined structure, facilitate insertion of the metallopeptide. Overall, the lack of metallopeptide interaction within the bulge of TAR RNA seemingly underscores the loop selectivity of these agents.

Summary. The site-selective cleavage of two native RNA substrates by low-molecular weight metallopeptides was investigated. As demonstrated through cleavage gel analyses, these metal complexes are capable of inducing the strand scission of the stem−loop regions of $tRNA^{Phe}$ and HIV-1 TAR RNA. The metallopeptides most likely react to cause initial nucleobase damage, followed by complete RNA strand scission with the aid of aniline acetate. The presence of structuring elements within these loops is suggested to affect their recognition; the metallopeptides may insert into a loop structure and sense its local environment in combination with the sequence of nucleobases it contains.

The ability of the metallopeptides to specifically recognize structural aspects of nucleic acids may assist in our development and understanding of nucleic acid-binding antitumor or antiviral agents. In addition, since the metallopeptides employed contain the same functional groups that nucleic acid-binding proteins utilize in their interactions with DNA and RNA, they can seemingly bridge the gap between artificial metal complexes and proteins in the study of RNA recognition phenomena. While other complexes seem to target the single-strandedness of an RNA, or other features, it appears as if the metallopeptides are actually sensitive to the local loop structure and/or sequence. In this regard, the metallopeptides mimic the activity of the majority of selective RNA-interacting proteins examined to date (*15*, *16*). A systematic exploitation of this metallopeptide property may eventually provide a means of predictably binding or cleaving RNA loop structures.

ACKNOWLEDGMENT

We thank Dr. David P. Mack (Parke-Davis Pharmaceutical Research) for samples of synthetic TAR RNA.

REFERENCES

1. Chow, C. S., and Bogden, F. M. (1997) *Chem. Rev. 97*, 1489−1513.
2. Pyle, A. M., and Barton, J. K. (1990) *Prog. Inorg. Chem. 38*, 413−475.
3. Sigman, D. S., Mazumber, A., and Perrin, D. M. (1993) *Chem. Rev. 93*, 2285−2316.
4. Hecht, S. M. (1994) *Bioconjugate Chem. 5*, 513−526.
5. Holmes, C. E., Abraham, A. T., Hecht, S. M., Florentz, C., and Giege, R. (1996) *Nucleic Acids Res. 24*, 3399−3406.
6. Holmes, C. E., Duff, R. J., van der Marel, G. H., van Boom, J. H., and Hecht, S. M. (1997) *Bioorg. Med. Chem. 5*, 1235−1248.
7. Chow, C. S., and Barton, J. K. (1990) *J. Am. Chem. Soc. 112*, 2839−2841.
8. Chow, C. S., Behlen, L. S., Uhlenbeck, O. C., and Barton, J. K. (1992) *Biochemistry 31*, 972−982.
9. Chen, X., Woodson, S. A., Burrows, C. J., and Rokita, S. E. (1993) *Biochemistry 32*, 7610−7616.
10. Burrows, C. J., and Rokita, S. E. (1996) *Met. Ions Biol. Syst. 33*, 537−560.
11. Murakawa, G. J., Chen, C.-H. B., Kuwabara, M. D., Nierlich, D. P., and Sigman, D. S. (1989) *Nucleic Acids Res. 17*, 5361−5375.
12. Liang, Q., Eason, P. D., and Long, E. C. (1995) *J. Am. Chem. Soc. 117*, 9625−9631.
13. Long, E. C., Eason, P. D., and Liang, Q. (1996) *Met. Ions Biol. Syst. 33*, 427−452.
14. Liang, Q., Ananias, D. C., and Long, E. C. (1998) *J. Am. Chem. Soc. 120*, 248−257.
15. Draper, D. E. (1995) *Annu. Rev. Biochem. 64*, 593−620.
16. Varani, G. (1997) *Acc. Chem. Res. 30*, 189−195.
17. Burrows, C. J., and Muller, J. G. (1998) *Chem. Rev. 98*, 1109−1151.
18. Stewart, J. M., and Young, J. D. (1984) in *Solid-Phase Peptide Synthesis*, Pierce Chemical Co., Rockford, IL.
19. Peattie, D. A. (1979) *Proc. Natl. Acad. Sci. U.S.A. 76*, 1760−1764.
20. Ehresmann, C., Baudin, F., Mougel, M., Romby, P., Ebel, J.-P., and Ehresmann, B. (1987) *Nucleic Acids Res. 15*, 9109−9129.
21. Lapidot, A., Ben-Asher, E., and Eisenstein, M. (1995) *FEBS Lett. 367*, 33−38.
22. Mei, H.-Y., Galan, A. A., Halim, N. S., Mack, D. P., Moreland, D. W., Sanders, K. B., Truong, H. N., and Czarnik, A. W. (1995) *Bioorg. Med. Chem. Lett. 5*, 2755−2760.
23. Neenhold, H. R., and Rana, T. M. (1995) *Biochemistry 34*, 6303−6309.
24. Kappen, L. S., and Goldberg, I. H. (1995) *Biochemistry 34*, 5997−6002.
25. Aboula-Ela, F., Karn, J., and Varani, G. (1995) *J. Mol. Biol. 253*, 313−332.
26. Brodsky, A. S., and Williamson, J. R. (1997) *J. Mol. Biol. 267*, 624−639.
27. Quigley, G. J., and Rich, A. (1976) *Science 194*, 796−806.
28. Rich, A. (1977) *Acc. Chem. Res. 10*, 388−396.
29. Churcher, M. J., Lamont, C., Hamy, F., Dingwall, C., Green, S. M., Lowe, A. D., Butler, J. G., Gait, M. J., and Karn, J. (1993) *J. Mol. Biol. 230*, 90−110.
30. Puglisi, J. D., Tan, R., Calnan, B. J., Frankel, A. D., and Williamson, J. R. (1992) *Science 257*, 76−80.
31. Calnan, B. J., Tidor, B., Biancalana, S., Hudson, D., and Frankel, A. D. (1991) *Science 252*, 1167−1171.
32. Tao, J., and Frankel, A. D. (1992) *Proc. Natl. Acad. Sci. U.S.A. 89*, 2723−2726.
33. Kim, S. H., Sussman, J. L., Suddath, F. L., Quigley, G. J., McPherson, A., Wang, A. H. J., Seeman, N. C., and Rich, A. (1974) *Proc. Natl. Acad. Sci. U.S.A. 71*, 4970−4974.
34. Westhof, E., Dumas, P., and Moras, D. (1985) *J. Mol. Biol. 184*, 119−145.
35. Sugiura, Y., Totsuka, R., Araki, M., and Okuno, Y. (1997) *Bioorg. Med. Chem. 5*, 1229−1234.
36. Jucker, F. W., and Pardi, A. (1995) *Biophys. Chem. 19*, 219−222.
37. Thorp, H. H., McKenzie, R. A., Lin, P.-N., Walden, W. F., and Theil, E. C. (1996) *Inorg. Chem. 35*, 2773−2779.
38. Carter, P. J., Cheng, C.-C., and Thorp, H. H. (1998) *J. Am. Chem. Soc. 120*, 632−642.
39. Loret, E., Georgel, P., Johnson, W. C., and Ho, P. S. (1992) *Proc. Natl. Acad. Sci. U.S.A. 89*, 9734−9738.
40. Jaeger, J. A., and Tinoco, I., Jr. (1993) *Biochemistry 32*, 12522−12530.
41. Weeks, K. M., and Crothers, D. M. (1991) *Cell 66*, 577−588.

BI9806605